Journal of Food Engineering 387 (2025) 112330

Contents lists available at ScienceDirect

Journal of Food Engineering

journal homepage: www.elsevier.com/locate/jfoodeng

Design of foodgrade oleofoams from carnauba wax and glyceryl monostearate whippable oleogels

Angela Borriello [a], Nicoletta Antonella Miele [a,*], Paolo Masi [a,b], Silvana Cavella [a,b]

[a] Department of Agricultural Sciences -University of Naples Federico II, Piazza Carlo di Borbone 1, 80055, Portici, Italy
[b] Center of Food Innovation and Development in the Food Industry, University of Naples Federico II, Via Università 100, 80055, Portici, Italy

ARTICLE INFO

Keywords:
Oleofoams
Oleogels
Natural wax
Rheological properties
Physical stability

ABSTRACT

The study aimed to design oleofoams based on carnauba wax (CW) and glyceryl monostearate (GMS), investigating the effect of their ratio (10:0, 8:2, 7:3, 6:4, 5:5, 4:6, 3:7, 2:8; 0:10) on the resulting oleofoam properties. Dynamic rheological analyses were performed to explore the mechanical properties of both oleogels and oleofoams. Oleofoams were also characterized for texture, color and physical stability Both oleogels and oleofoams exhibited a solid-like behaviour confirming the formation of a fat crystal network during the cooling and whipping process. Oleogels with lower G′ values generated the most stable oleofoams. CW-based oleogel did not whip, while GMS-based oleofoam did not show desirable properties. A CW: GMS ratio of 3:7, 4:6, or 5:5 is required to obtain self-standing oleogels with high oil binding capacity, whippable in 25–40 min reaching an overrun of 50%. The resulting oleofoams are stable and characterized by high network strength, crucial for food applications.

1. Introduction

The oleogelation is a common method of plasticizing an oil using molecules that self-assemble into a 3D network forming viscoelastic and thermoreversible structures called oleogels (Sabet et al., 2023). Oleogels have been extensively studied as substitutes for solid fats and successfully applied in many health food products (Santos et al., 2023; Zhao et al., 2020; Borriello et al., 2022a).

Among oleogelators, monoglycerides (MAGs) are the most studied ones, due to both safety and efficient structuring ability (Valoppi et al., 2017; Ferro et al., 2019; Li et al., 2021). However, the use of bio-oleogelators, such as natural waxes, represents a suitable alternative in terms of costs and efficiency.

In recent years, novel fat-based aeration systems called “oleofoams” have gained attention for their enhanced role in reducing solid fat content in aerated food products, such as sponge cakes, mousse and aerated sauces (Fameau and Saint-Jalmes, 2020; Saremnejad et al., 2020).

Oleofoam is a non-aqueous foam, so its formulation requires less or no preservatives, aligning with the food industry trend toward “clean label” product development (Hu and Meng, 2023). Indeed, oleofoam development is more challenging than hydrated foams due to the limited surface activity of several edible emulsifiers at the oil–air interface.

Oleofoams are generally obtained through mechanical whipping of an oleogel, because depressurization is also used but it determines unstable foams (Gunes et al., 2017). Oleogel aeration can only be achieved within a certain range of crystalline concentration; at low content, there are not enough fat crystals to stabilize the foam, while too many crystals form a very hard oleogel that is difficult to aerate. During mechanical whipping, part of the crystals of the oleogel is adsorbed on the air bubble surface, meanwhile, the excess crystals remain in the continuous phase forming a network that reduces the possibility of oil drainage and bubble dissolution so stable foams are obtained (Hu and Meng, 2023).

Oleofoams can be prepared with several types of compounds, used alone or in combinations; MAGs are also used as oleofoam stabilizers (Gunes et al., 2017; Heymans et al., 2018; Du et al., 2021; Grossi et al., 2023; Hussein Alhasan, Mazaheri Tehrani and Varidi, 2024; Saha et al., 2020; Tirgarian et al., 2023; Tirgarian and Farmani, 2023) at a concentration of ≈10% (w/w). Among different MAGs, Glyceryl monostearate (GMS) is the most used one. To improve physical and thermal stability of GMS-based oleofoams, some authors suggested to increase GMS concentration up to 20% (Tirgarian et al., 2023), but a graininess sensation was reported, or combine it with other agents (Saha et al., 2020; Truong et al., 2019; Hossein Goli et al., 2023; Tirgarian and

* Corresponding author.
E-mail address: nicolettaantonella.miele@unina.it (N.A. Miele).

https://doi.org/10.1016/j.jfoodeng.2024.112330
Received 7 February 2024; Received in revised form 9 September 2024; Accepted 22 September 2024
Available online 26 September 2024

Farmani, 2023). The combination or partial substitution of GMS with a wax could improve the interfacial elasticity and the strength of the continuous oleogel phase providing high stability to the resulting oleofoam. Saha et al. (2020) used paraffin and synthetic waxes in sunflower oil to develop oleofoams. They reported that the wax layer covering the bubble surface reduced the surface tension and imparted an interfacial elasticity exercising a stabilizing effect, but this was not able to arrest the bubble dissolution. The bulk elasticity of the oleogel surrounding the bubbles appeared to mostly contribute to the stability of the system.

As reported by Truong et al. (2019), the combination of GMS with phytosterol determined oleofoams with lower elasticity and foam stability than that containing GMS alone, because a better crystalline network with small crystals was formed in the oleogel. A double network oleogelation system, made of glycerol monostearate and a soy-protein isolate-polysaccharides conjugate, was also recently proposed by Tirgarian and Farmani (2023), but the resulting oleofoams were not thermoreversible. Hossein Goli et al., 2023 showed that the co-crystallization of MAG and beeswax (BW) determined stable oleofoams, by using a mixture of BW: GMS (1:1 w/w), at 12.5%. They also highlighted the importance of future studies on establishing the link between the rheological properties of the oleogel and that of associated oleofoam to design novel oleofoam for different food applications.

The current study aimed to design novel and stable oleofoams by whipping oleogels made with sunflower oil and two different oleogelators, GMS, and carnauba wax (CW), varying their ratio. GMS can gel a vegetable oil through the creation of inverse lamellar phase stabilized by hydrogen bonds, meanwhile wax forms a tridimensional network in which crystals and their aggregates block the liquid oil through van der Waals interactions (Malvano et al., 2024). CW is a natural wax already used to prepare oleogels, at a concentration varying from 4 to 10% (Ögütcüa and Yılmaz, 2014; Tanislav et al., 2022; Borriello et al., 2022a; Bastürk et al., 2023). GMS: CW combination was recently explored, in different ratios and concentrations, to gel canola oil, obtaining oleogels with improved properties than those of GMS oleogel (Pakseresht et al., 2023), but no information was reported on whipping ability of those combinations. To find the appropriate CW: GMS ratio for whippable oleogels, first nine oleogels were prepared by changing the ratios of CW and GMS from 10:0 to 0:10, at a fixed oleogelator concentration of 10%, and were characterized in terms of rheological, and colorimetric properties as well as oil binding capacity. Then, whipping ability of oleogels was assessed by collecting overrun and colorimetric measurements during whipping process. Finally, rheological behavior, textural analysis and physical stability of oleofoams were also investigated.

2. Materials and methods

2.1. Materials

Sunflower oil (SO) was purchased from MePa alimentari srl (Pozzuoli, Italy). Micronized carnauba wax (CW, melting point of 80–85 °C) was donated by a local candy company. Glyceryl monostearate (GMS, pH 9.5, melting point of 56–62 °C, purity degree 97%) was purchased from Flower Tales srl (Milan, Italy).

2.2. Oleogel preparation

CW and GMS were used to gel SO at a fixed concentration (10%). A total of 9 oleogels were prepared by changing the CW: GMS ratios (10:0, 8:2, 7:3, 6:4, 5:5, 4:6, 3:7, 2:8; 0:10). The mixture oil/oleogelator was stirred at 200 rpm using a magnetic stirrer for 5 min at 80 °C, until a clear solution was obtained. The samples were then cooled to 8 °C for 12 h and kept for 1 h at 25 °C before the whipping. Two productions for each oleogel were carried out. For each production, at least three replications of all the analyses were performed.

2.3. Oil binding capacity

Oil binding capacity (OBC), the percentage of liquid oil trapped inside the gel structure after applying a given centrifugal force, was determined as reported in Borriello et al. (2021) with some modifications. Oleogel-forming solution (10 ml) was placed into tared tubes and stored at ambient temperature overnight for full gelation. The tubes were weighed and centrifuged at 10,000 rpm for 15 min using a centrifuge (HERMLE Z 326 K). The excess oil was drained, and the tubes were weighed again. OBC was calculated as in the following equation:

$$OBC\ (\%) = x\left[1 - \frac{(m_1 - m_2)}{m_1}\right] \times 100 \quad (1)$$

where m1 and m2 are the mass of the initial and final samples (after centrifugation), respectively. Five replicates were performed for each sample.

2.4. Foaming process and overrun measurement

Oleofoams were obtained by whipping at 25 °C 100 g of oleogel in a glass bowl (15 cm diameter) with a hand-held electric mixer at speed position 3 (i.e., 300 rpm) equipped with two whisks. Oleogels were whipped for different times (from 5 to 60 min) to collect overrun measurements, while for all the other analyses, each oleogel was whipped until the maximum overrun. Two productions for each oleofoam were carried out. For each production, at least three replications of all the analyses were performed. All samples were stored in an incubator at 25 °C for 1 h for subsequent analysis unless specified otherwise.

The overrun (θ) was calculated to investigate the whipping ability, as reported by Brun et al. (2015), according to the following equation:

$$\theta = \frac{Vair}{Vair + Voil} \quad (2)$$

where $Vair + Voil$ corresponds to the volume of the foam, and $Voil$ is the volume of the oil after keeping the foam at 80 °C. The measurements were conducted in triplicate at 25 °C.

2.5. Rheology

Rheological measurements were carried out with a Modular Advanced Rheometer System (HAAKE MARS, ThermoScientific, Waltham, USA), equipped with parallel plate geometry (d = 30 mm, 2.0 mm gap). Strain sweep (σ from 0.01 to 100 %, ω = 1 Hz) and frequency sweep (ω from 0.1 to 100 Hz, σ within the LVR) tests were performed on both oleogels and oleofoams. The flow and thixotropic behaviors were also investigated for the oleofoam samples with desired whipping and rheological properties (3:7, 4:6, 5:5, 6:4, 7:3 and 8:2). The viscosity curves were measured as a function of the increasing shear rate (1–100 s^{-1}) and also determined at alternating low and high shear rates, (shear rate of 0.1 s^{-1} for 500 s, at 10 s^{-1} for 300 s, at 0.1 s^{-1} for 500 s). The measurements were conducted in triplicate at 25 °C.

2.6. Texture analysis

A TMS-Pro (Food Technology Corporation) texturometer equipped with a 50 N load cell was used to measure the firmness (maximum force during penetration) of the foams. The oleofoams were poured into plastic containers (5 cm diameter, 3 cm height) and equilibrated at 25 °C. A PMMA (Plexiglass) cylindrical probe (diameter 2.5 cm) was used to perform a penetration test. The cylinder penetrated the sample at a crosshead speed of 120 mm/min up to a depth of 10 mm, corresponding to about 50 % of the initial height of the sample. Finally, five independent tests were performed for each sample.

2.7. Color

A colorimeter (Minolta Chroma Meter, CR 300, Japan) was used to determine the color of both oleogels and oleofoams. The Hunter parameters L* (from 0 = black to 100 = white), a* (-a* = greenness to + a* = redness), and b* (-b* = blueness to + b* = yellowness) were measured and averaged from three randomly positions for each sample. The total color difference (Δ E) was calculated according to the following equation:

$$\Delta E = \sqrt{\Delta L^2 + \Delta a^2 + \Delta b^2} \quad (3)$$

where Δ L, Δ a*, Δ b* are the differentials between oleogels and the sunflower oil and between oleofoam and respective oleogel color parameters.

2.8. Turbiscan stability

A Turbiscan Tower stability analyser (Formulaction, France) was used to evaluate the physical stability of oleofoam during storage time. Specific cylindrical glass tubes for sample coring were used to obtain the same height (≈45 mm) for all samples and not to damage the foam structure. Oleofoam were scanned for 2 months at 25 °C. Stability of samples was expressed in terms of Turbiscan Stability Index (TSI), which is defined as follows:

$$TSI = \frac{\sum_i \sum_h |scan_i\ (h) - scan_{i-1}\ (h)|}{N_h} \quad (4)$$

where $scan_i(h)$ is the light intensity of the scan acquired at the i-th time instant and at a height of h, and N_h is the number of height positions in the selected scanning zone of the tube (Wang et al., 2018; Cavella et al., 2020). The data were analysed by using the software package TowerSoft Ver 1.2 (Formulaction, France). Three replicates were performed for each sample.

2.9. Data analysis

The stress at the limit of linearity (τ_0), as the stress where G′ value decreased by more than 10% of the values recorded in the LVR, and yield stress (τ^*), as the stress where the storage and loss moduli are equal (G′ = G″), were determined from strain sweep curves (Dinkgreve et al., 2016). Data were reported as the difference between τ_0 and τ^* ($\Delta\tau$).

The frequency curves were fitted according to the rheological Power Law model which is represented in the following equation:

$$G' = a(\omega)^b \quad (5)$$

where G′ is the storage modulus (Pa), ω is the frequency (Hz), and a (Pa·s^b) and b (−) are parameters used to describe rheological behaviour. Modelling of the thixotropic behaviour of oleofoam was performed applied a first-order stress decay models with a non-zero stress value as in the following equation:

$$\tau - \tau_{eq} = (\tau_i - \tau_{eq})\ e^{-kt} \quad (6)$$

where τ_i, τ_{eq} and k are the initial shear stress value, the equilibrium stress value and the breakdown rate constant, respectively.

Univariate analysis of variance (ANOVA) and multiple comparisons of means (Duncan's test, $p \leq 0.05$) were performed to evaluate whether differences among the samples, due to the different CW:GMS ratio, were statistically significant ($p \leq 0.05$) by using SPSS for Windows version 17.0 (SPSS Inc., Chicago, IL, USA).

3. Results and discussion

3.1. Oleogel characterization

All the samples showed a solid-like behaviour as the elastic moduli (G′) were larger than the viscous ones (G″) within the LVR (Fig. 1a and **b**), then both moduli gradually decreased up to a point where external stress overcame the non-covalent forces of the three-dimensional network of oleogels which assumed a liquid-like behaviour. At low strain percentages, single component-based oleogels presented the lowest (GMS) and the highest (CW) G′ values, respectively. Ögütcüa and Yılmaz (2014) found that CW-based oleogels were firmer than those made with GMS, by means of texture analysis results. The CW: GMS-based oleogels 2:8, 3:7, 4:6 and 5:5 showed lower G′ values (≈70000 Pa) than the oleogels 8:2 (≈120000 Pa), 7:3 (≈175000 Pa), and 6:4 (≈228000 Pa) (Fig. 1a–b). G′ and G″ moduli in LVR, and the difference between the stress at the limit of linearity and the yield stress ($\Delta\tau$) are reported in Table 1. Oleogels 0:10, 2:8 and 3:7 showed low $\Delta\tau$ values, which correspond to a short distance between τ_0 and τ^*, suggesting the presence of equal magnitude intermolecular forces which breakdown simultaneously at low strain values. Intermediate (10:0, 4:6, 5:5, and 8:2 CW: GMS-based oleogels) and high (6:4, 7:3 CW: GMS-based oleogels) $\Delta\tau$ values observed, on the other hand, indicated that the breaking of the forces occurred at various times, confirming the presence of different magnitudes bonds and a more connected structure able to withstand under greater deformations. All the oleogels behaved as solid-like materials since only a slight frequency dependence of G′ moduli was observed (Fig. 1c–**d**). The parameters "*a*" and "*b*" estimated by fitting frequency curves with the power law model (eq. 5) are reported in Table 1. The lowest values of the parameter "*b*" were observed for 3:7 and 4:6 oleogels, which were 0.03 and 0.07, respectively, revealing their stronger structures. Meanwhile, for the other oleogels, no significant differences were observed, showing "*b*" values close to 0.1, according to values observed by Borriello et al. (2022a) for oleogels made up of sunflower oil and CW. The oleogels containing a higher amount of CW and a small amount of GMS (6:4, 7:3 and 8:2) showed high values of the parameter "*a*", which reached the maximum value for the sample 6:4 (386619 Pa·s^b). Similarly, "*a*" values, close to 183000 Pa·s^b, were observed for mono-component oleogels 0:10 and 10:0. Mechanical spectra and the fitting parameters, which assumed gel-like values, suggested that all the oleogels had a strong network. Our results are comparable with those observed in our previous work, in which CW based oleogels showed storage modulus values (from frequency sweep) ranging from 10^5 to 10^6 Pa (Borriello et al., 2022b). The combination of CW and GMS determined oleogels with a self-standing structure and a good tolerance to deformation rate. Moreover, our results are in accordance with those reported by Pakseresht and co-authors (2023); they showed that small and even-distributed crystals were formed in canola oleogels in which CW: GMS ratio was in favor of CW, but at inverted ratios, CW inclusion reduced the structuring effect of GMS, determined less interconnected oleogels.

The oleogel CW: GMS 0:10 and 10:0 showed the lowest and the highest oil binding capacity, 75.29% and 97.77%, respectively (**Table 1**). These results indicated that GMS alone or combined with small wax concentrations (2:8; 3:7; 4:6), gave a limited oil binding capacity to oleogel, and the addition of CW was required to obtain excellent OBC. Furthermore, the 5:5, 6:4 and 7:3 ratio oleogels behaved like 10:0 oleogels, indicating a synergistic effect for specific CW: GMS ratios. Those results are in line with those of Pakseresht et al. (2023).

Comparable results were also found by Öğütcü et al. (2015), as fish oil oleogel produced with MG showed lower OBC than those of sunflower wax. Li et al. (2021) reported that poor OBC of GMS oleogels depended on the presence of spherical crystals with a low capacity to bind oil, as well as reported also by Da Pieve et al. (2010).

The color of oleogels may impact their food-related application. Some investigators reported that not only oil but also the oleogelator

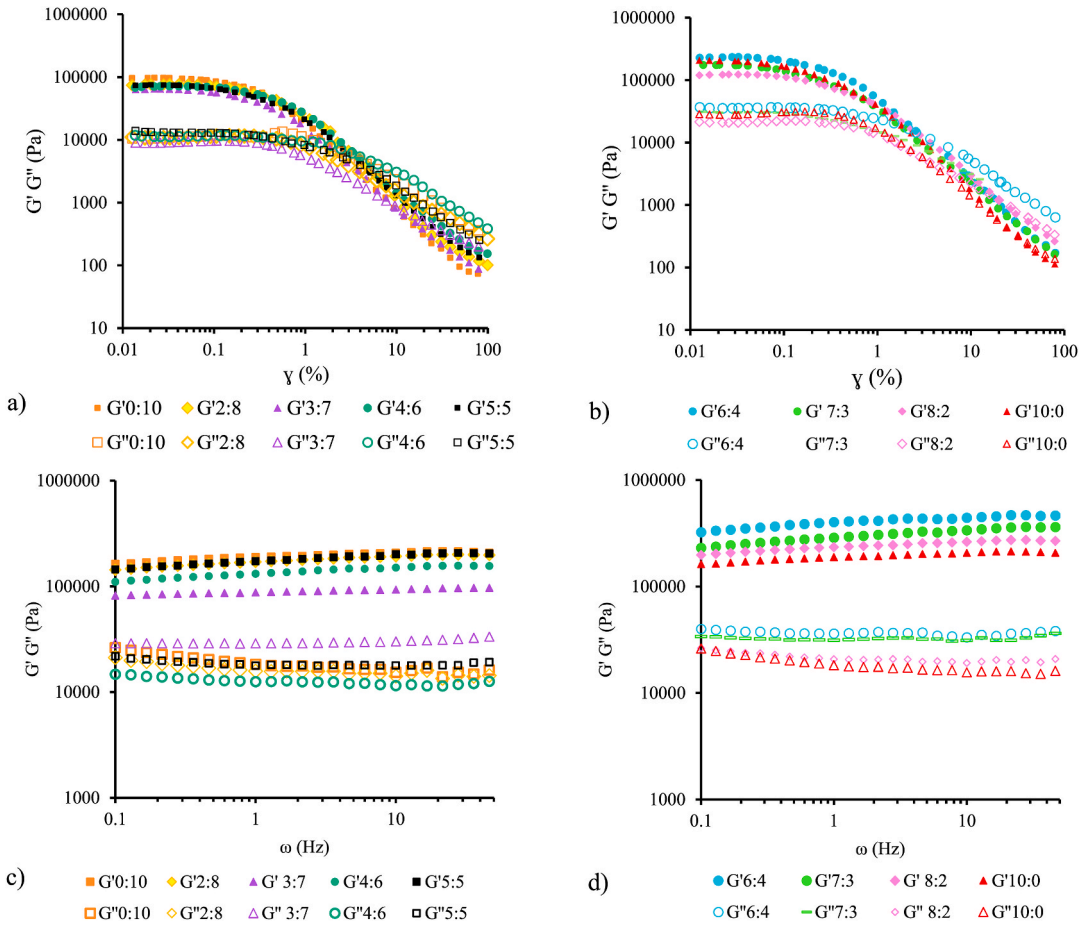

Fig. 1. Mechanical properties of oleogels. Strain sweep (a and b) and frequency sweep (c and d) curves of oleogels with different CW: GMS ratios.

Table 1
Oleogels physical characterization. Elastic (G′) and viscous (G″) moduli in LVR, and the difference (Δτ) between stress at the limit of linearity and the yield stress determined by strain sweep test; the parameters "*a*" and "*b*" estimated by fitting frequency curves with the power law model ($G' = a\omega^b$); oil binding capacity (OBC %); color parameters (ΔE calculated with respect to the colorimetric parameters of sunflower oil) of oleogels with different CW: GMS ratios.

	G' (Pa)	G'' (Pa)	Δτ (Pa)	a (Pa·s^b)	b (−)	R^2	OBC (%)	ΔE
0:10	95150 ± 1808^{bc}	10608 ± 1241^{c}	87.74 ± 9.83^{c}	183001 ± 7131^{c}	0.09 ± 0.00^{a}	0.95	75.29 ± 0.28^{c}	18.98 ± 0.52^{c}
2:8	71426 ± 1462^{c}	9962 ± 2684^{c}	97.95 ± 7.70^{c}	166982 ± 24396^{cd}	0.09 ± 0.00^{a}	0.92	87.32 ± 0.50^{b}	21.85 ± 0.57^{bc}
3:7	61237 ± 2378^{c}	6997 ± 1966^{c}	94.91 ± 9.66^{c}	87251 ± 976^{e}	0.03 ± 0.00^{c}	0.96	90.79 ± 0.29^{ab}	18.60 ± 0.85^{c}
4:6	64004 ± 1911^{c}	8887 ± 2016^{c}	154.25 ± 23.12^{b}	130052 ± 19804^{d}	0.07 ± 0.00^{b}	0.96	92.32 ± 2.07^{ab}	26.78 ± 0.48^{b}
5:5	68828 ± 1121^{c}	11661 ± 1522^{c}	192.36 ± 16.11^{b}	169741 ± 1637^{cd}	0.10 ± 0.00^{a}	0.93	96.22 ± 1.19^{a}	22.56 ± 1.14^{bc}
6:4	220740 ± 2448^{a}	35863 ± 3390^{a}	301.2 ± 25.32^{a}	386619 ± 101086^{a}	0.09 ± 0.00^{a}	0.93	96.30 ± 0.58^{a}	24.32 ± 0.36^{b}
7:3	175623 ± 5480^{ab}	28891 ± 1055^{ab}	304.10 ± 19.24^{a}	283011 ± 7972^{b}	0.10 ± 0.00^{a}	0.96	96.81 ± 0.15^{a}	22.52 ± 0.26^{bc}
8:2	128944 ± 5442^{b}	18977 ± 352^{b}	203.13 ± 16.21^{ab}	229643 ± 57257^{b}	0.09 ± 0.00^{a}	0.91	95.07 ± 2.02^{a}	22.31 ± 0.24^{bc}
10:0	206161 ± 1039^{ab}	28657 ± 1034^{ab}	131.91 ± 19.86^{b}	183068 ± 7179^{c}	0.09 ± 0.00^{a}	0.96	97.77 ± 1.36^{a}	30.53 ± 0.82^{a}

For each column, different letters correspond to significantly different values ($p \leq 0.05$) from Duncan's test.

type may affect the optical properties of oleogels (Malvano et al., 2024; Borriello et al., 2022b). In our work, oleogels with higher content of GMS showed a creamy-white color, whereas CW seemed to have a greater impact on the yellowness and greenness. Therefore, all samples are potentially suitable for food application. Moreover, the color differences between the sunflower oil and the oleogels (ΔE) were visible to the naked eye (**Table 1**). The oleogels appeared more opaque than sunflower oil, mainly due to the change in structure induced by the sol/gel transition. The lightness generally decreased with the oleogelation, because the crystalline network had a lower refractive index than that of the oil. Less refraction of light through more compact structures resulted in a lighter color (Moghtadaei et al., 2018).

3.2. Whipping ability

The overrun (%) as a function of whipping time (min) was determined to investigate the foamability of oleogels at different CW: GMS ratios (Fig. 2). The best whipping performance was observed for sample 3:7, which had an overrun of 50% after 25 min of whipping. The samples 0:10, 2:8, 4:6 and 5:5 also showed high overrun (50%) after 40, 35, 35 and 30 min of whipping, respectively. An overrun value of 40% was reached after 40 and 25 min for 6:4 and 7:3, respectively. An oleofoam which retains 40–50 % air (oleogel-based), could be used in low-calorie lipid-based products, such as aerated fillings (Tirgarian and Farmani, 2023), or an aerated reduced-fat sauce (Saremnejad et al., 2020). The 8:2 sample performed differently, as the overrun reached a maximum value of 26% after only 15 min, seemed to remain constant for future

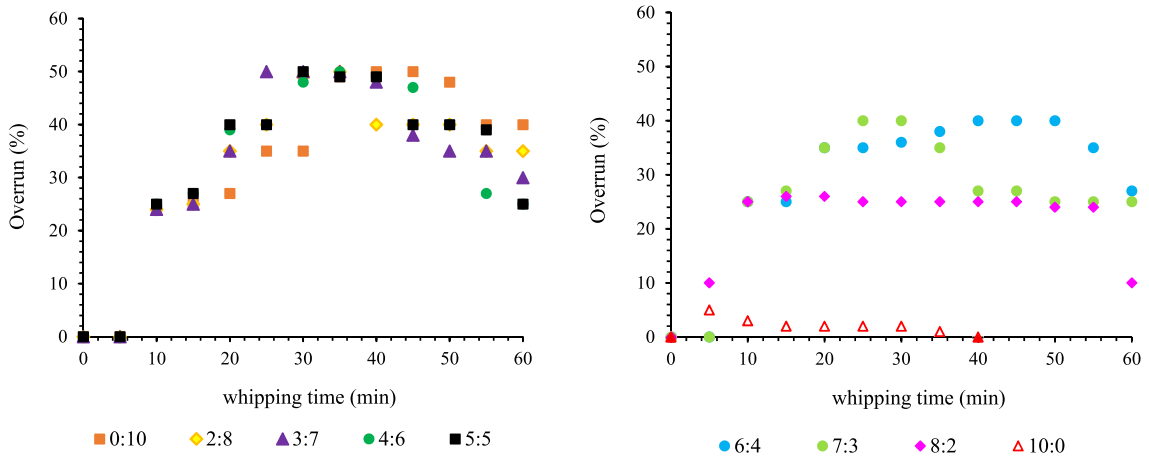

Fig. 2. Whipping ability. Overrun as a function of whipping time of oleofoams with different CW: GMS ratios.

whipping times, and suddenly decreased after 60 min. The overrun values ≈ 50% are in accordance with those reported by Gunes et al. (2017) and Truong et al. (2019) for oleofoams made by whipping MAG-based oleogels. Those low overrun values depend on the mechanism of foaming, which relies on pre-formed crystals stabilizing the air bubbles in the oily continuous phase. Due to packing constraints at higher volume fractions, air bubbles tend to coalesce and get out, so the amount of air incorporated is usually lower than that of an aqueous system. However, whipping ability is affected by oleogel type, in terms of MAG and oil used, thus, even higher overrun values (≈200%) could be obtained by mechanical whipping of an oleogel (Grossi et al., 2023).

Our results showed that all the oleogels containing MAG were whippable even if they differed for maximum overrun and whipping time to reach it. The 10:0 sample, which did not whip, was then eliminated from further analyses and discussions. These results were quite expected considering the air-oil interface stabilization effect of MAG

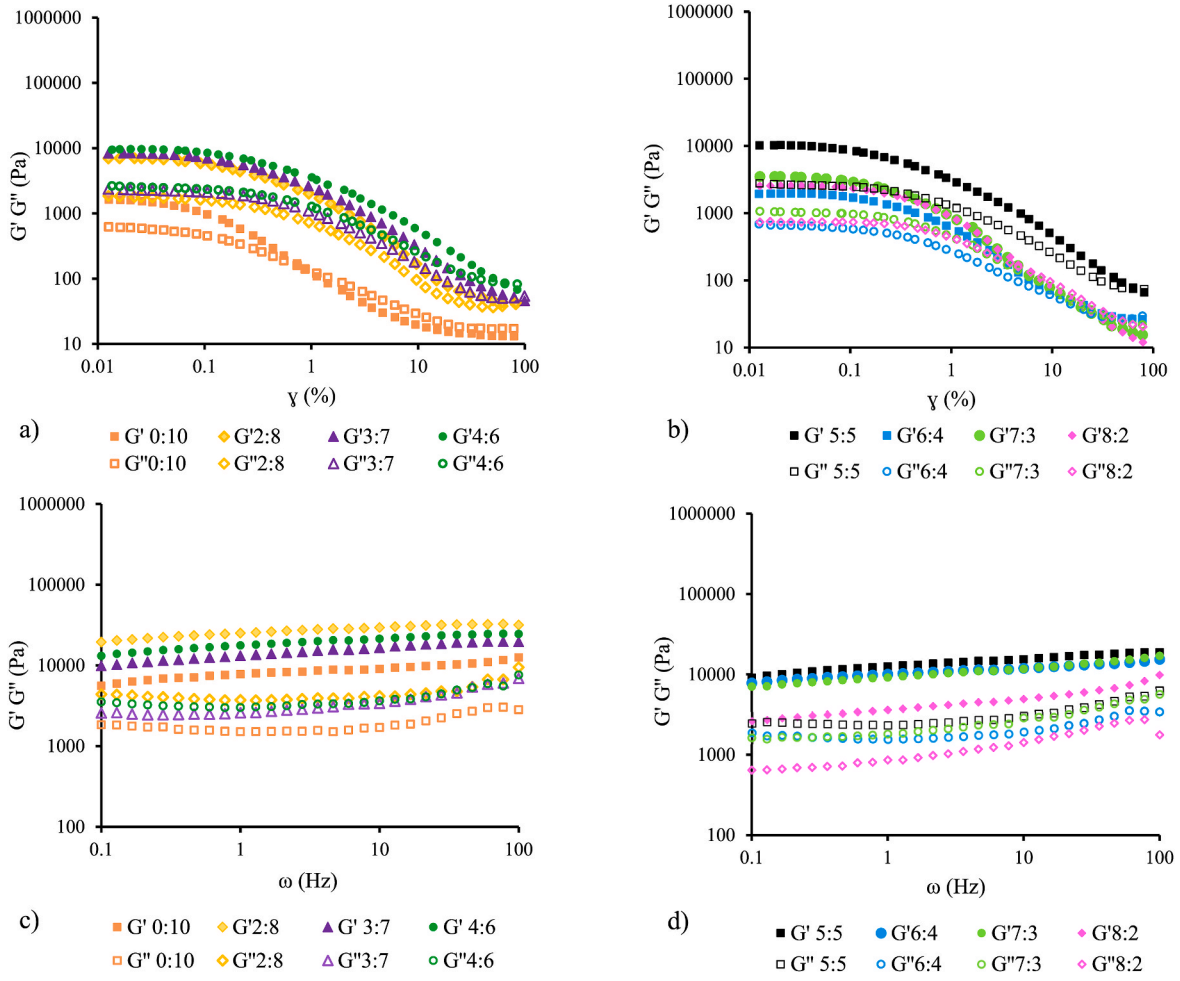

Fig. 3. Mechanical properties of oleofoams. Strain sweep (a and b) and frequency sweep (c and d) curves of oleofoam with different CW: GMS ratios.

crystals (Mohanan et al., 2022), due to their Pickering effect on air bubbles at the interface, and the difficulty of whipping wax-based oleogels (Mohanan et al., 2020). However, oleogels made by using a combination of MAG and wax presented desirable properties, affecting the properties of the resulting oleofoams.

Results highlighted that whipping parameters were influenced by G' modulus, the Δτ and the OBC of the oleogels. It is known from the literature that oleogels with G′ in the range 10^3–10^8 Pa allowed air incorporation, making the foaming possible (Gunes et al., 2017), and oleofoam aeration can be achieved only in a specific range of crystalline concentrations, as well as rheological properties (Metilli et al., 2022). Our oleogels were all in the range reported by Gunes et al. (2017), with differences in G′ and Δτ depending on CW: GMS ratio that affected whipping abilities.

Whipping abilities of the oleogel are also related to its OBC, with a positive correlation between oleogel OBC and oleofoam overrun. Our results showed that the addition of specific amount of wax (samples 4:6 and 5:5) generated an increase in the OBC values of the oleogels (**Table 1**) and the overrun of the oleofoams (Fig. 2). A further increase in wax concentration did not influence the OBC, but the system became too viscous to be able to include air. Our results agreed with those reported by Callau et al. (2020) for oleofoams prepared with stearic acid and stearyl alcohol in sunflower oil.

3.3. Oleofoam characterization

3.3.1. Oleofoam rheological properties

The rheological properties of the oleofoams are reported in Fig. 3. In Table 2 G', G″ moduli in LVR, Δτ, "*a*" and "*b*", ΔE and the firmness of oleofoams are listed. The strain sweep curves displayed a typical gel-like profile for all the oleofoams, with the storage modulus being higher than the loss ones until they crossed over when a certain percentage of deformation was reached. Both the air-oil interface crystalline layers (interfacial contribution) and the oleogel three-dimensional network in the lamellae (mass stabilization) contributed to the viscoelastic behavior of the oleofoams (Heymans et al., 2018). Nevertheless, many differences in terms of network strength (G′ in LVR) were found between the samples. The samples 5:5 and 4:6 showed the highest G′ value (≈10000 Pa), followed by 3:7 and 2:8 (=8371 and 6998 Pa, respectively), meanwhile for the other samples no significant differences were observed in terms of elastic modulus in the LVR.

Oleofoams made from oleogel with 0:10 ratio showed the lowest value of Δτ (≈1 Pa) suggesting that GMS alone, although was able to generate well-structured oleogels (Fig. 1a and **c**), was not suitable to produce strong and stable oleofoams. The initial oleogel (0:10) was not stable to oil loss, as shown by the lowest OBC (**Table 1**) and released free liquid oil during the whipping process resulting in a weak foam that required lower shear stress to flow. Δτ values increased with increasing wax concentration up to maximum values close to 60 Pa for oleofoams 4:6 and 5:5, while they decreased with further additions of wax. Oleofoams containing considerable amounts of wax also showed extremely low Δτ values (8:2, 7:3, and 6:4) suggesting that in these samples all bonds break with equal force. These results agreed with those related to the oleogels oil binding capacity and whipping ability. Specific CW: GMS ratios are required to obtain oleogels with OBCs that facilitate air inclusion and obtain oleofoams with higher intermolecular forces. Regarding the time-dependent deformation phenomena, the solid-like behaviour of oleofoam dominated over different observation times since the elastic modulus was always higher than the viscous ones (Fig. 3c and **d**). The elastic moduli slightly depended on the frequency and the power-law model well-fitted their curves ($R^2 > 0.93$). Obviously, the parameters "*a*" and "*b*" estimated for oleofoams (**Table 2**) were lower than those estimated for oleogels (**Table 1**). A large variability between samples was found in terms of parameter "*a*", which ranged from 3500 to 24000 Pa·s^b. The oleofoam 5:5, 7:3 and 8:2 showed the lowest "*b*" values (=0.13 ± 0.02), following by 2:8, 3:7, 6:4 and 4:6 (≈0.17). The highest "*b*" value (=0.21) was observed for oleofoam 0:10 showing the greatest frequency dependence and confirming the weak nature of this system.

These results suggested that stronger oleogels (par.3.1), showing high G′ values in LVR, gave oleofoams with low network strength, and the reverse was also true. Indeed, a certain amount of crystals is needed to make oleofoam. If the network is weak, unstable foam can form and if the network is too firm, the system is not able to produce foam. Moreover, the greater the strength of the oleofoam network, the greater the shear stress required to flow, and our results agreed with the findings of Heymans et al. (2018). They observed the highest foamability in oleogels that exhibited lower G′ moduli in which crystallization was still ongoing. On the other hand, Gunes et al. (2017) reported a lower air incorporation in oleogel with a lower elastic modulus.

The greatest differences in terms of color between the oleofoam and respective oleogel (ΔE) were observed for the sample 4:6 (ΔE = 38.74). No relationship was found between the values of ΔE and the overrun. However, the lightness of the oleofoams (L*) rapidly increased within 10 min of whipping, after which it increased more slowly up to the maximum overrun value, and then decreased slightly. Observed differences in L* values during whipping time between samples reflect the ability of the oleogel to trap a different amount of air (Fig. S1- supplementary materials). Higher lightness values during whipping were observed for the 5:5 sample, followed by 3:7, 4:6 and 6:4, for which there were no differences, while the 8:2 sample showed the lowest L* values.

All the oleofoams were self-standing and the greatest firmness values were obtained for samples 4:6 and 5:5 (2.38 and 2.42 N, respectively), followed by 3:7, 6:4 and 2:8 (≈1.9 ± 0.1), 0:10 and 7:3 (=1.78 and 1.31N), and the lowest value (=0.76 N) for the sample 8:2. The oleogels which included higher amounts of air in shorter times gave foams with higher firmness values. Furthermore, Callau et al. (2020) highlighted that firmer oleofoams could be obtained by whipping oleogels containing mixed crystals, supporting the presence of synergy between CW

Table 2
Oleofoam physical characterization. Elastic (G′) and viscous (G″) moduli in LVR, and the difference (Δτ) between stress the stress at the limit of linearity (τ_0) and the yield stress (τ^*) determined by strain sweep test; the parameters "*a*" and "*b*" estimated by fitting frequency curves with the power law model ($G' = a\omega^b$); color parameters (ΔE calculated with respect to the colorimetric parameters of respective oleogel) and firmness (N) of oleofoam with different CW:GMS ratios.

	G' (Pa)	G″ (Pa)	Δτ (Pa)	a (Pa·s^b)	b (–)	R^2	ΔE	Firmness (N)
0:10	1149 ± 86^c	561 ± 14^c	1.11 ± 0.68^d	7262 ± 1952^c	0.21 ± 0.02^a	0.94	32.22 ± 0.60^c	1.78 ± 0.01^b
2:8	6998 ± 46^b	1778 ± 148^b	43.92 ± 2.84^b	24081 ± 1110^a	0.16 ± 0.00^{ab}	0.95	35.03 ± 0.25^b	1.86 ± 0.01^b
3:7	8371 ± 54^b	1659 ± 126^b	48.48 ± 0.45^b	12831 ± 691^b	0.17 ± 0.00^{ab}	0.93	31.03 ± 0.56^d	1.93 ± 0.19^b
4:6	9955 ± 49^a	2215 ± 55^a	64.83 ± 4.34^a	16889 ± 528^{ab}	0.18 ± 0.00^{ab}	0.97	38.74 ± 0.17^a	2.38 ± 0.26^a
5:5	10403 ± 62^a	1947 ± 15^a	62.01 ± 0.79^a	12386 ± 2208^b	0.11 ± 0.01^c	0.98	35.90 ± 0.76^b	2.42 ± 0.08^a
6:4	1701 ± 11^c	460 ± 11^c	20.33 ± 0.31^c	9698 ± 2829^{bc}	0.16 ± 0.03^{ab}	0.96	35.94 ± 0.06^b	1.91 ± 0.01^b
7:3	3426 ± 14^c	944 ± 17^c	7.52 ± 0.12^d	9022 ± 137^{bc}	0.13 ± 0.01^b	0.97	35.85 ± 0.18^b	1.31 ± 0.04^c
8:2	2386 ± 15^c	570 ± 33^c	7.00 ± 1.21^d	3598 ± 245^d	0.15 ± 0.01^b	0.98	30.49 ± 0.58^d	0.76 ± 0.01^d
10:0	–	–	–	–	–	–	–	–

For each column, different letters correspond to significantly different values ($p \leq 0.05$) from Duncan's test.

and GMS in overrun and firmness increasing.

The flow (Fig. 4a) and thixotropic (Fig. 4b) behaviors were studied for multi-component samples that showed high overrun and short whipping times (3:7, 4:6, 5:5, 6:4, 7:3); sample 8:2 was also added as a negative example. The oleofoams behaved as shear-thinning fluids, at the lowest shear rate (1 s^{-1}) the differences among the curves were the greatest, meanwhile the viscosities slightly differed at the highest shear rate (100 s^{-1}). 3:7 and 8:2 samples showed the highest and lowest viscosity value (86.21 and 32.80 Pa s) respectively, while samples 4:6, 5:5, 6:4 and 7:3 showed similar viscosity curves.

Thixotropy represents an important rheological property to be taken into consideration for the potential application of oleofoams in food processing. At constant low and high shear rates all the oleofoams showed a time-dependant behavior as the viscosity slowly decreased with increasing time (Fig. 4b). The sudden increase of shear rate from 0.1 s^{-1} to 10 s^{-1} induced a significant decrease of the viscosity displaying the shear-thinning behavior. When the shear rate rapidly decreased at 0.1 s^{-1} the oleofoam viscosity instantly grew up showing a structure recovery, from 20% to 67% with increasing CW content.

The first-order stress decay model with a non-zero steady state stress value well fitted shear stress–time data ($R^2 > 0.97$) and the results of modelling are shown in Table 3. For all the samples τ_i increased with increasing the shear rate from 0.1 to 10 s^{-1} and then decreased returning to 0.1 s^{-1}. The parameter τ_{eq} seemed to follow a similar trend except for the sample 3:7 which showed an increase of τ_{eq} value going from low to high shear rates.

The parameter k, a measure of thixotropic breakdown rate, increased with increasing shear rate and it still increased when the shear rate decreased to 0.1 s^{-1} suggesting that the breakdown rate of oleofoams under a shear field accelerated at high shear rates. At a low shear rate, the greatest difference due to the composition was observed in terms of τ_{eq} that decreased with increasing CW concentration. At a high shear rate, the same behavior was observed for τ_i, τ_{eq} and k, which decreased as CW increased from 190.69 Pa to 54.37 Pa, from 82.75 Pa to 33.96 Pa and from 0.026 to 0.006 s^{-1}, respectively.

The recovery rate (%), calculated considering τ_{eq} ((τ_{eq} 0.1*s^{-1}/τ_{eq} 0.1s^{-1})x100), was affected by CW: GMS ratio ranging from 20 to 74%, for 3:7 and 7:3, respectively (Fig. S2 of supplementary files).

3.3.2. Oleofoam stability

In Fig. 5 Turbiscan stability index (TSI) at the meniscus as a function of storage time for the samples 3:7, 4:6, 5:5, 6:4, 7:3 and 8:2 was reported. Samples 6:4 and 7:3 showed an increasing trend within 63 days, reaching TSI values close to 43.9 and 38.2, respectively, resulting in the less stable ones. Samples 5:5 and 4:6 showed a similar trend that rapidly increased in the first week, then the growth rate slowed down until assuming an almost constant trend. The most stable sample was 3:7 which reached the lowest TSI values as early as 40 days of storage. The 8:2 sample has anomalous behavior, as well as whipping ability, as it reached a TSI value like that of the 5:5 sample (=28) after 48 days but showed an increasing linear trend which suggested instability of the sample for future storage times. The most stable foams were those showing both high G′ values in the LVR and the best whipping performance. In samples that showed higher strength (i.e. higher G′ LVR) the

Table 3
The parameters estimated by fitting shear stress–time data with a first-order stress decay model with a non-zero equilibrium stress value (eq. 5).

	$\dot{\gamma}$ (s^{-1})	τ_i (Pa)	τ_{eq} (Pa)	k (s^{-1})	R^2
3:7	0.1	176.527 ± 30.358^{b}	124.125 ± 4.260^{a}	0.006 ± 0.003^{c}	0.992
	10	190.698 ± 6.077^{b}	82.756 ± 2.151^{b}	0.026 ± 0.004^{b}	0.974
	0.1*	48.680 ± 2.076^{c}	24.996 ± 0.338^{c}	0.022 ± 0.005^{bc}	0.974
4:6	0.1	57.783 ± 9.947^{b}	52.855 ± 7.199^{b}	0.009 ± 0.00^{c}	0.986
	10	148.694 ± 4.621^{a}	72.677 ± 2.283^{a}	0.027 ± 0.00^{a}	0.982
	0.1*	28.842 ± 1.769^{c}	19.190 ± 1.590^{c}	0.017 ± 0.00^{b}	0.990
5:5	0.1	51.401 ± 4.060^{b}	35.198 ± 2.289^{b}	0.010 ± 0.00^{c}	0.978
	10	123.991 ± 4.125^{a}	67.005 ± 1.322^{a}	0.015 ± 0.00^{b}	0.971
	0.1*	39.339 ± 1.557^{c}	17.387 ± 0.377^{c}	0.026 ± 0.00^{a}	0.989
6:4	0.1	68.182 ± 3.775^{c}	49.439 ± 1.963^{b}	0.010 ± 0.00^{c}	0.984
	10	129.613 ± 4.272^{b}	72.858 ± 1.552^{a}	0.013 ± 0.00^{b}	0.985
	0.1*	67.745 ± 4.705^{c}	29.996 ± 1.883^{c}	0.017 ± 0.00^{a}	0.985
7:3	0.1	52.185 ± 6.410^{c}	32.352 ± 5.677^{b}	0.005 ± 0.00^{ac}	0.987
	10	106.822 ± 5.695^{b}	66.678 ± 2.831^{a}	0.013 ± 0.00^{b}	0.975
	0.1*	45.797 ± 6.540^{c}	24.175 ± 1.472^{c}	0.026 ± 0.00^{a}	0.972
8:2	0.1	23.5456 ± 2.441^{c}	10.8234 ± 0.853^{b}	0.003 ± 0.00^{c}	0.996
	10	54.3744 ± 2.098^{b}	33.9698 ± 0.826^{a}	0.006 ± 0.00^{b}	0.996
	0.1*	19.5564 ± 0.399^{c}	7.0531 ± 1.083^{c}	0.014 ± 0.00^{a}	0.994

For each sample, in each column, different letters correspond to significantly different values ($p \leq 0.05$) from Duncan's test.
01* = share rate applied after 10 s^{-1} for 300 s.

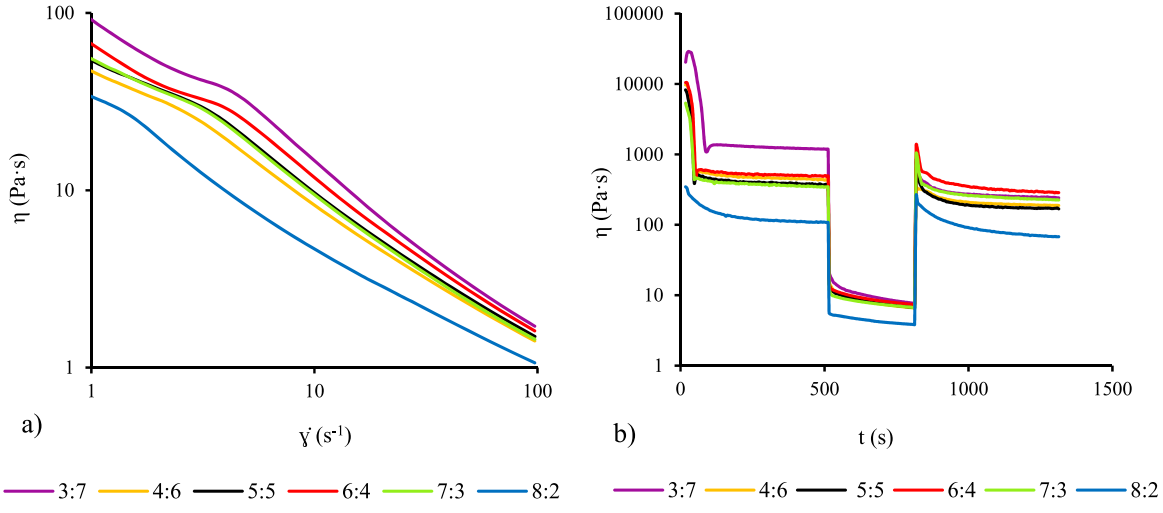

Fig. 4. Flow and thixotropic behaviour. Viscosity as a function of shear rate (a) and shearing time, $\dot{\gamma}$ = 0.1 and 10 s^{-1}, (b) of oleofoams with different CW: GMS ratios.

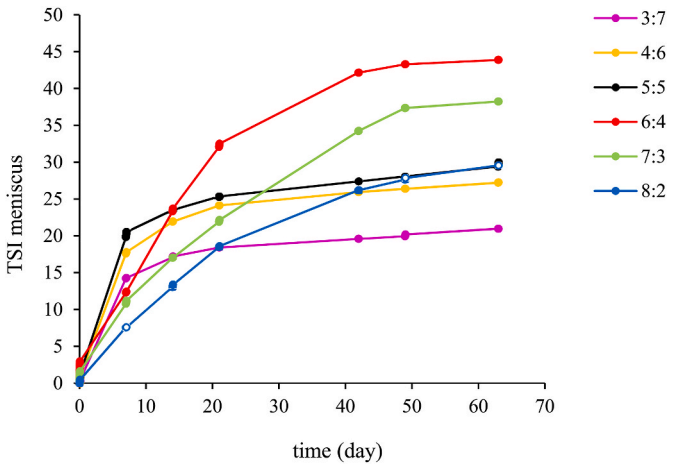

Fig. 5. Destabilization kinetic. Evolution of turbiscan stability index (TSI) over time for oleofoam with different CW: GMS ratios.

crystals generated a firmer network in the continuous phase which affected the stability of oleofoams.

4. Conclusions

Oleofoams are very promising for the food industry, and it is of interest the impact of formulation on oleofoam properties. Our results showed that a self-standing oleogel could be obtained by using only GMS or CW as oleogelator for sunflower oil, but CW-based oleogel did not whip, while GMS-based oleofoam did not show desirable properties. The combination of CW and GMS determined oleogels that could be whipped in 25–40 min reaching an overrun of 50%. Stronger oleogels gave oleofoams with low network strength, and the reverse was also true. Oleogels that showed lower G′ values entrapped more air due to their lower viscosity and generated the most stable oleofoams which showed both high G′ values in the LVR and the best whipping performance, with a CW: GMS ratio of 3:7, 4:6, or 5:5. These results may provide useful and practical information for the applications of CW: GMS based oleogels and relative oleofoams in food formulation. By choosing the right CW: GMS ratio it is possible to obtain tailored functionalities for specific food applications.

This study has also some limitations, further detailed investigation was required to better understand the relationship between the microstructure of the oleogels, in terms of type and dimensions of crystals, and the resulting structure of the oleofoams, in terms of distribution, shape and dimensions of air bubbles.

CRediT authorship contribution statement

Angela Borriello: Writing – review & editing, Writing – original draft, Visualization, Investigation, Formal analysis. **Nicoletta Antonella Miele:** Writing – review & editing, Writing – original draft, Visualization, Investigation, Conceptualization. **Paolo Masi:** Writing – review & editing, Project administration. **Silvana Cavella:** Writing – review & editing, Writing – original draft, Validation, Supervision, Project administration, Conceptualization.

Declaration of competing interest

The authors declare that they have no known competing financial interests or personal relationships that could have appeared to influence the work reported in this paper.

Data availability

Data will be made available on request.

Appendix A. Supplementary data

Supplementary data to this article can be found online at https://doi.org/10.1016/j.jfoodeng.2024.112330.

References

Bastürk, A., Badem, Ş., Ceylan, M.M., 2023. Propolis and carnauba wax-based safflower oil oleogels as fat substitutes in cakes: production, oxidative stability, and characterization. Eur. J. Lipid Sci. Technol. 125, 2200213.
Borriello, A., Masi, P., Cavella, S., 2021. Novel pumpkin seed oil-based oleogels: development and physical characterization. LWT - Food Sci. Technol. (Lebensmittel-Wissenschaft -Technol.) 152, 112165.
Borriello, A., Miele, N.A., Masi, P., Cavella, S., 2022a. Rheological properties, particle size distribution and physical stability of novel refined pumpkin seed oil creams with oleogel and lucuma powder. Foods 11 (13), 1844.
Borriello, A., Miele, N.A., Masi, P., Aiello, A., Cavella, S., 2022b. Effect of fatty acid composition of vegetable oils on crystallization and gelation kinetics of oleogels based on natural wax. Food Chem. 375, 131805.
Brun, M., Delample, M., Harte, E., Lecomte, S., Leal-Calderon, F., 2015. Stabilization of air bubbles in oil by surfactant crystals: a route to produce air-in-oil foams and air-in-oil-in-water emulsions. Food Res. Int. 67, 366–375.
Callau, M., Sow-Kébé, K., Jenkins, N., Fameau, A.L., 2020. Effect of the ratio between fatty alcohol and fatty acid on foaming properties of whipped oleogels. Food Chem. 333, 127403.
Cavella, S., Miele, N.A., Fidaleo, M., Borriello, A., Masi, P., 2020. Evolution of particle size distribution, flow behaviour and stability during mill ball refining of a white chocolate flavouring paste. LWT - Food Sci. Technol. (Lebensmittel-Wissenschaft -Technol.) 132, 109910.
Da Pieve, S., Calligaris, S., Co, E., Nicoli, M.C., Marangoni, A.G., 2010. Shear nanostructuring of monoglyceride organogels. Food Biophys. 5, 211–217.
Dinkgreve, M., Paredes, J., Denn, M.M., Bonn, D., 2016. On different ways of measuring "the" yield stress. J. Non-Newtonian Fluid Mech. 238, 233–241.
Du, L., Jiang, Q., Li, S., Zhou, Q., Tan, Y., Meng, Z., 2021. Microstructure evolution and partial coalescence in the whipping process of oleofoams stabilized by monoglycerides. Food Hydrocolloids 112, 106245.
Fameau, A.L., Saint-Jalmes, A., 2020. Recent advances in understanding and use of oleofoams. Front. Sustain. Food Syst. 4, 110.
Ferro, A.C., Okuro, P.K., Badan, A.P., Cunha, R.L., 2019. Role of the oil on glyceryl monostearate based oleogels. Food Res. Int. 120, 610–619.
Grossi, M., Fang, B., Rao, J., Chen, B., 2023. Oleofoams stabilized by monoacylglycerides: impact of chain length and concentration. Food Res. Int. 169, 112914.
Gunes, D.Z., Murith, M., Godefroid, J., Pelloux, C., Deyber, H., Schafer, O., Breton, O., 2017. Oleofoams: properties of crystal-coated bubbles from whipped oleogels-evidence for pickering stabilization. Langmuir 33 (6), 1563–1575.
Heymans, R., Tavernier, I., Danthine, S., Rimaux, T., Van der Meeren, P., Dewettinck, K., 2018. Food-grade monoglyceride oil foams: the effect of tempering on foamability, foam stability and rheological properties. Food Funct. 9 (6), 3143–3154.
Hossein Goli, S.A., Rezvani, M., Abdollahi, M., 2023. Beeswax and monoglycerol-based oil foam: effect of oil type and oleogelator concentration on physicochemical, rheological properties and storage stability. Food Struct. 37, 100343.
Hu, X., Meng, Z., 2023. An overview of edible foams in food and modern cuisine: destabilization and stabilization mechanisms and applications. Compr. Rev. Food Sci. Food Saf. 23, e13284.
Hussein Alhasan, F., Mazaheri Tehrani, M., Varidi, M., 2024. Producing superior oleofoams: unraveling the impact of oil type, surfactant concentration, and production temperature on foam stability and functional characteristics. Food Chem. X 21, 101033.
Li, J., Guo, R., Bi, Y., Zhang, H., Xu, X., 2021. Comprehensive evaluation of saturated monoglycerides for the forming of oleogels. LWT - Food Sci. Technol. (Lebensmittel-Wissenschaft -Technol.) 151, 112061.
Malvano, F., Albanese, D., Cinquanta, L., Liparoti, S., Marra, F., 2024. A comparative study between beeswax and glycerol monostearate for food-grade oleogels. Gels 10, 214.
Metilli, L., Lazidis, A., Francis, M., Marty-Terrade, S., Ray, J., Simone, E., 2022. Application of X-ray microcomputed tomography for the static and dynamic characterization of the microstructure of oleofoams. Cryst. Growth Des. 21 (3), 1562–1575.
Moghtadaei, M., Soltanizadeh, N., Goli, S.A.H., 2018. Production of sesame oil oleogels based on beeswax and application as partial substitutes of animal fat in beef burger. Food Res. Int. 108, 368–377.
Mohanan, A., Nickerson, M.T., Ghosh, S., 2020. The effect of addition of high-melting monoacylglycerol and candelilla wax on pea and Faba bean protein foam-templated oleogelation. J. Am. Oil Chem. Soc. 97 (12), 1319–1333.
Mohanan, A., Harrison, K., Cooper, D.M., Nickerson, M.T., Ghosh, S., 2022. Conversion of pulse protein foam-templated oleogels into oleofoams for improved baking application. Foods 11 (18), 2887.

Ögütcü, M., Yılmaz, E., 2014. Oleogels of virgin olive oil with carnauba wax and monoglyceride as spreadable products. Grasas Aceites 65 (3), e040.
Öğütcü, M., Temizkan, R., Arifoğlu, N., Yılmaz, E., 2015. Structure and stability of fish oil organogels prepared with sunflower wax and monoglyceride. J. Oleo Sci. 64 (7), 713–720.
Pakseresht, S., Tehrani, M.M., Farhoosh, R., Koocheki, A., 2023. The monoglyceride oleogel characteristics modified by carnauba wax. LWT - Food Sci. Technol. (Lebensmittel-Wissenschaft -Technol.) 185, 115156.
Sabet, S., Pinto, T.C., Kirjoranta, S.J., Kazerani Garcia, A., Valoppi, F., 2023. Clustering of oleogel production methods reveals pitfalls and advantages for sustainable, upscalable, and oxidative stable oleogels. J. Food Eng. 357, 111659.
Saha, S., Saint-Michel, B., Leynes, V., Binks, B.P., Garbin, V., 2020. Stability of bubbles in wax-based oleofoams: decoupling the effects of bulk oleogel rheology and interfacial rheology. Rheol. Acta 59, 255–266.
Santos, M.A.S., Magalhães, A.E.R., Okuro, P.K., Steel, C.J., Cunha, L.R., 2023. High internal phase emulsion-template oleogels stabilized by sodium caseinate:quercetin complexes and potential application in pound cakes. J. Food Eng. 366, 111860.
Saremnejad, F., Mohebbi, M., Koocheki, A., 2020. Practical application of nonaqueous foam in the preparation of a novel aerated reduced-fat sauce. Food Bioprod. Process. 119, 216–225.
Tanislav, A.E., Puşcaş, A., Păucean, A., Mureş, A.E., Semeniuc, C.A., Mureşan, V., Mudura, E., 2022. Evaluation of structural behavior in the process dynamics of oleogel-based tender dough products. Gels 8, 317.
Tirgarian and Farmani, 2023. A novel approach for the development of edible oleofoams using double network oleogelation systems. Food Chem. 426, 136634.
Tirgarian, B., Yadegari, H., Bagheri, A., Neshagaran, E., Mardani, M., Farmani, J., 2023. Reduced-fat chocolate spreads developed by water-in-oleogel emulsions. J. Food Eng. 337, 111233.
Truong, T., Prakash, S., Bhandari, B., 2019. Effects of crystallisation of native phytosterols and monoacylglycerols on foaming properties of whipped oleogels. Food Chem. 285, 86–93.
Valoppi, F., Calligaris, S., Barba, L., Šegatin, N., Poklar Ulrih, N., Nicoli, M.C., 2017. Influence of oil type on formation, structure, thermal, and physical properties of monoglyceride-based organogel. Eur. J. Lipid Sci. Technol. 119 (2), 1500549.
Wang, K., Li, G., Zhang, B., 2018. Opposite results of emulsion stability evaluated by the TSI and the phase separation proportion. Colloids Surf. A Physicochem. Eng. Asp. 558, 402–409.
Zhao, M., Lan, Y., Cui, L., Monono, E., Rao, J., Chen, B., 2020. Formation, characterization, and potential food application of rice bran wax oleogels: expeller-pressed corn germ oil versus refined corn oil. Food Chem. 309, 125704.